Benign Synthesis of 2-Ethylhexanoic Acid by Cytochrome P450cam: Enzymatic, Crystallographic, and Theoretical Studies†

Kevin J. French,‡ Michael D. Strickler,‖ Dan A. Rock,§ Denise A. Rock,§ Grace A. Bennett,§ Jan L. Wahlstrom,§ Barry M. Goldstein,‖ and Jeffrey P. Jones*,§

Toxicology Training Program, Department of Environmental Medicine, and Department of Biochemistry and Biophysics, University of Rochester School of Medicine and Dentistry, Rochester, New York 14642, and Department of Chemistry, Washington State University, Pullman, Washington, 99164

Received January 9, 2001; Revised Manuscript Received June 1, 2001

ABSTRACT: This study examines the ability of P450cam to catalyze the formation of 2-ethylhexanoic acid from 2-ethylhexanol relative to its activity on the natural substrate camphor. As is the case for camphor, the P450cam exhibits stereoselectivity for binding (*R*)- and (*S*)-2-ethylhexanol. Kinetic studies indicate (*R*)-2-ethylhexanoic acid is produced 3.5 times as fast as the (*S*)-enantiomer. In a racemic mixture of 2-ethylhexanol, P450cam produces 50% more (*R*)-2-ethylhexanoic acid than (*S*)-2-ethylhexanoic acid. The reason for stereoselective 2-ethylhexanoic acid production is seen in regioselectivity assays, where (*R*)-2-ethylhexanoic acid comprises 50% of total products while (*S*)-2-ethylhexanoic acid comprises only 13%. (*R*)- and (*S*)-2-ethylhexanol exhibit similar characteristics with respect to the amount of oxygen and reducing equivalents consumed, however, with (*S*)-2-ethylhexanol turnover producing more water than the (*R*)-enantiomer. Crystallographic studies of P450cam with (*R*)- or (*S*)-2-ethylhexanoic acid suggest that the (*R*)-enantiomer binds in a more ordered state. These results indicate that wild-type P450cam displays stereoselectivity toward 2-ethylhexanoic acid synthesis, providing a platform for rational active site design.

Cytochrome P450[1] is a superfamily of heme containing enzymes that catalyze the reduction of oxygen to a reactive monooxygen species responsible for a wide variety of chemical reactions. Present in almost all organisms from bacteria to plants to mammals, there are currently over 700 known isoforms (*1*). Cytochrome P450s catalyze oxidation reactions in the biosynthesis of vitamins, steroids, fatty acids, and other endogenous compounds. Another important role of these enzymes is in detoxifying xenobiotics. Many P450 isoforms are located where exposure to foreign compounds occurs frequently, such as the lung and liver. These qualities give cytochrome P450s the capacity to metabolize a broad range of hydrophobic substrates, facilitating their clearance.

Cytochrome P450cam (CYP 101) is a soluble, monomeric isoform from *Pseudomonas putida* that catalyzes the first step of converting (*R*)-camphor into a food source. P450cam uses molecular oxygen, two protons, and two electrons to produce 5-exohydroxycamphor, with water as a byproduct.

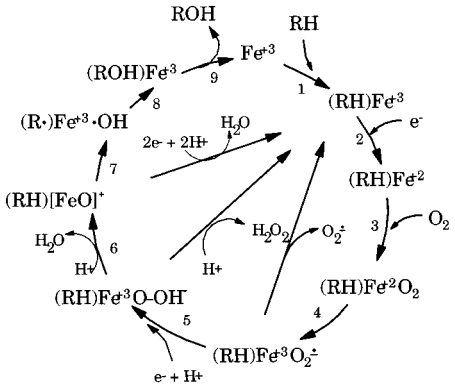

FIGURE 1: The catalytic cycle. Divergent reactions in the center depict potential mechanisms of uncoupling.

Over 25 years of research have shown that this mechanism occurs through a series of steps collectively called the catalytic cycle, which is depicted in Figure 1 (*2*). The plethora of knowledge available for this enzyme makes it an attractive model for biotechnological applications. One field of interest is benign synthesis, the production of a chemical through safer means. Enzymatic synthesis may provide a benign replacement for industrial oxidation methods, which use toxic and carcinogenic heavy metal reactants to perform these reactions. Biocatalysts offer a cleaner and possibly more efficient process using mild, biological conditions while potentially performing regioselective and stereoselective reactions. Herein we report data pertaining to the use of P450cam in the oxidation of 2-ethylhexanol to 2-ethylhexanoic acid (Figure 2).

† This work was supported by National Science Foundation Grant 9710129 (J.P.J. and B.M.G.) and the National Institute of Environmental Health Sciences' University of Rochester Toxicology Training Grant ES07026 (K.J.F.) and ES0 09122 (J.P.J.).

* To whom correspondence should be addressed at Department of Chemistry, Washington State University, Pullman, Washington, 99164, Telephone 509-335-5983, Fax 509-335-8867, E-mail jpj@wsu.edu.

‡ Toxicology Training Program, Department of Environmental Medicine, University of Rochester School of Medicine and Dentistry.

‖ Department of Biochemistry and Biophysics, University of Rochester School of Medicine and Dentistry.

§ Washington State University.

[1] Abbreviations: P450, cytochrome P450; DEHP, diethylhexylphthlate; GC-MS, gas chromatography−mass spectroscopy; NMR, nuclear magnetic resonance; Amax, maximum absorption.

10.1021/bi010063+ CCC: $20.00
Published on Web 07/17/2001

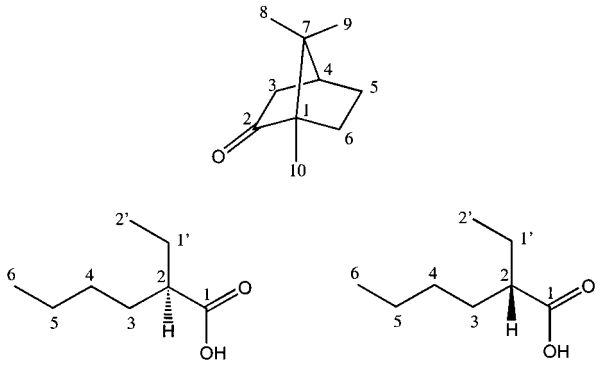

FIGURE 2: (1*R*)-Camphor (center), (*R*)-2-ethylhexanoic acid (left), and (*S*)-2-ethylhexanoic acid (right).

2-Ethylhexanoic acid is a versatile and industrially important carboxylic acid, having been used use as a resin, fungicide, lubricant, and detergent (*3*). However, the most important role of 2-ethylhexanoic acid is not as an industrial product, but as a major metabolite of di-2-ethylhexylphthalate or DEHP. DEHP is the most commonly used plasticizer for poly(vinyl chloride) products (*4*) and is a ubiquitous environmental pollutant. Human exposure to DEHP occurs through the environment or ingestion from foodstuffs or medical containers that leach DEHP over time (*5*). Upon ingestion, esterases hydrolyze DEHP to 2-ethylhexanol, which is then oxidized to 2-ethylhexanoic acid by P450s in the liver (*6*). Mouse studies have shown racemic 2-ethylhexanoic acid to cause peroxisome proliferation (*7*), while the (*R*)-enantiomer was discovered to be a potent teratogen, causing a myriad of birth defects in mice (*7*). Interestingly, (*S*)-2-ethylhexanoic acid showed no teratogenic effects, making it a safer chemical (*8*). Current industrial methods produce racemic mixtures. Therefore, 2-ethylhexanoic acid production through biocatalysis could bypass the use of toxic reactants, and potentially provide some sort of stereoselectivity, making both a safer catalyst and chemical.

Here we present findings that show P450cam produces 2-ethylhexanoic acid from 2-ethylhexanol in a stereoselective fashion. This ability of wild-type P450cam to perform regioselective and stereoselective catalysis provides a starting point for future active site design directed toward a more efficient biocatalyst.

MATERIALS AND METHODS

Chemicals and Reagents. All solvents were purchased from J. T. Baker, Inc. (Phillipsburg, NJ). Chemicals were purchased from Aldrich Chemical Co. (Milwaukee, WI) with the following exceptions: MTBSTFA (+1% *tert*-butyldimethylchlorosilane) was purchased from Regis Technologies, Inc. (Morton Grove, IL), and potassium phosphate dibasic and monobasic and magnesium sulfate were from EM Science. Enzymes and cofactors were purchased from Sigma (St. Louis, MO). All synthesized compounds were compared and found to be consistent with the purchased, known compound or reported literature values with respect to NMR and GC/MS characteristics.

Synthesis of Optically Pure (R)- and (S)-2-Ethylhexanol and 2-Ethylhexanoic Acid. The methodology for synthesizing optically pure 2-ethylhexanoic acid was derived from Macherey (*9*). Gas chromatography/mass spectrometry and proton NMR confirmed the purity and identity of the product. The diastereomers were separated via gravity flow silica gel chromatography using an ethyl acetate/hexane mobile phase gradient of from 5 to 100% ethyl acetate. After hydrolysis the optical rotation was +3.7 degrees and −11.5 degrees, for the (*S*)-enantiomers and the (*R*)-2-ethylhexanoic acid respectively in agreement with the literature values (*9*).

Enzyme Expression and Purification. The enzymes where expressed and purified by the procedure of Shimoji et al. (*10*). After expression and purification, homogeneity for putidaredoxin and putidaredoxin reductase was confirmed by spectral analysis and SDS−PAGE (*11*).

Binding Assays. A 1 mL volume of 0.5 μM P450cam in 50 mM potassium phosphate buffer with 200 mM potassium chloride, pH 7.4, was titrated with aliquots of either camphor, *R*- and *S*-enantiomers of 2-ethylhexanol, or their corresponding enantiomers of 2-ethylhexanoic acid. Optical spectra in the region of 350 to 450 nm were measured using a SLM DW2000 UV−Vis spectrophotometer. All assays displayed a maximum absorbency at 388 nm and a minimum at 426 nm. The difference spectra were analyzed as a function of concentration of substrate using Graph Pad Prism linear regression to yield ΔA_{max} and K_S values.

V/K and Regioselectivity Studies. A typical enzymatic incubation consisted of 0.5 μM wild-type cytochrome P450cam, 1.0 μM putidaredoxin reductase, 5.0 μM putidaredoxin, an NADH regenerating system consisting of 35 U Type II L-lactate dehydrogenase, 25 mM L-lactate, 1 mM NADH, and varying concentrations of racemic, (*R*)-, or (*S*)-2-ethylhexanol or (*R*)-camphor in a reaction buffer of 50 mM potassium phosphate with 200 mM potassium chloride, pH 7.4. Control reactions consisted of identical samples without P450cam or the reducing enzymes. The incubations were carried out at 30 °C in a Dubnoff metabolic shaker and started by the addition of substrate. Reactions were terminated at 30 min with 3 mL of chloroform and 0.5 mL of 10% hydrochloric acid. An internal standard, 1-octanoic acid for 2-ethylhexanoic acid or 5-exonorcamphane for 5-exo-hydroxycamphor, was then added. The reactions were extracted with 3 × 3 mL of chloroform, dried with magnesium sulfate, and concentrated under nitrogen. The samples were derivatized MTBSTFA + 1% t-BCDMS (Regis). For the regioselective assays, the samples were analyzed without derivitization. Samples were injected into a Hewlett-Packard model 5972 gas chromatograph/mass spectrometer containing a Hewlett-Packard HP-1 capillary column. All samples were run in splitless mode. The gas chromatograph temperature started at 50 °C for 0.5 min, then increased to 150 °C at 10 °C per minute, and finally to 250 °C at 30 °C/min.

Enantiomeric Excess Assays. Incubations and extractions were carried out under saturating substrate conditions as described above. Samples were derivatized with diazomethane. An Rt-βDEXsm fused silica column (30m, 0.25 mm ID, Restek) was used at 60 °C for 1 min followed by a temperature ramp of 2 °C/min to 200 °C. (*S*)-Methyl-2-ethylhexanoate was detected at 15.9 min, while (*R*)-methyl-2-ethylhexanoate was detected at 16.1 min with baseline resolution.

Stoichiometric Analysis. Incubations were conducted as described above. NADH consumption was determined by monitoring the decrease in absorbance at 340 nm using a Hewlett-Packard UV−Vis spectrophotometer. Oxygen con-

sumption was determined using an ISO2 dissolved oxygen meter (World Precision Instruments). Peroxide formation was determined by adding 1000 U of catalase (Sigma) at the end of the reaction and calculating the increase of dissolved molecular oxygen. Reactions were terminated with either 4 mL of chloroform or 4 mL of ethyl acetate, extracted three times with 3 mL, dried with magnesium sulfate, concentrated, and analyzed as described above. All reactions were run at least in triplicate. Water production was determined by the equation $H_2O = [NADH - (ROH + H_2O_2)]/2$, where ROH equals the amount of hydroxylated product formed.

X-ray Crystallography. The enzyme purified as described above was further purified by a strong anion-exchange step using the PerSeptive Biosystems BioCAD Sprint system (Perkin-Elmer). Crystals of P450cam were grown using the sitting-drop vapor diffusion method from a reservoir solution of the above buffer plus 16−24% w/v poly(ethylene glycol), molecular weight 8000. Each drop contained 2 μL of 20−30 mg/mL protein and 2 μL of reservoir solution. Crystals were soaked for ∼1 h in a pH 7.0 cryoprotectant solution containing 50 mM potassium phosphate, 250 mM potassium chloride, 1 mM dithiothreitol, and 3 mM sodium (*S*)- or (*R*)-2-ethylhexanoate, and 30% poly(ethylene glycol), average weight 400. Crystals were then loop mounted and flash cooled to −170 °C using a MSC nitrogen cold stream. The data sets were collected at the University of Rochester using a R-AXIS II imaging plate system and Cu K_α radiation produced by a Rigaku rotation anode RU200 operated at 50 kV and 100 mA. All indexing and scaling were carried out using the HKL software package (*12*).

The models were phased using refined coordinates from a previous P450cam data set, which was initially phased from coordinates for the tetragonal form of P450cam, kindly provided by Dr. Ilme Schlichting, EMBL Heidelberg (*13*). This model did not include the first nine or the last two residues of the histidine-tagged protein, due to disorder at the N- and C-termini. In the case of the (*S*)-enantiomer structure, a change in space group necessitated molecular replacement methods using AmoRe from CCP4 version 3.3. Refinements were performed with maximum-likelihood methodology (*14*) using CNS version 5.0 (*15*).

Ab Initio Quantum Mechanical Calculations. Chemical structures for the reactants and products were constructed using SYBYL. Ground-state energies for reactants and products were calculated using GAUSSIAN 94 (*16*). Gas-phase transition state calculations were performed with GAUSSIAN 94 at the MP2 level of theory using the 6-31+G* basis set. Transition states were confirmed by the presence of one large negative harmonic frequency in a force calculation. $\Delta E^{\ddagger}$ for each reaction was calculated by subtracting the ground-state energies of reactants from the transition state energy.

Molecular Dynamic Simulations. The P450cam-(*S*)-2-ethylhexanol starting structure was derived from X-ray crystallographic data described above. Substrate bond lengths and angles, including the C−H−O transition bond, were obtained from the quantum mechanical ab initio calculations described above. The atomic charges of the substrate were calculated using the RESP program (*17*). Large force constants were placed on the C−H−O bonds to preserve the conditions of the transition state. The enzyme was then enclosed in a shell of waters, minimized using SANDER of the AMBER v. 4.1 program suite, (*17*) and equilibrated as described previously (*18*).

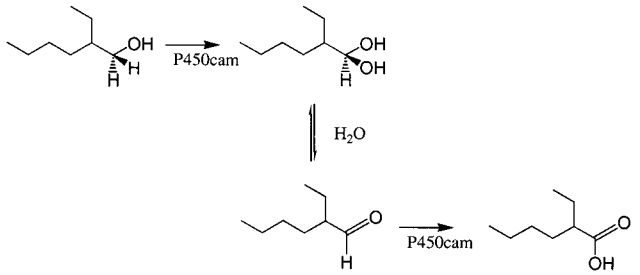

FIGURE 3: Proposed mechanism of 2-ethylhexanoic acid formation by cytochrome P450cam.

Table 1: Spectral Binding Data for Cytochrome P450cam[a]

substrate	K_s (μM)	Amax (AU/μM P450)	% high spin heme
camphor	0.79(2)	0.111(3)	100
(*R*)-2-ethylhexanol	63(1)	0.035(1)	32
(*S*)-2-ethylhexanol	130(1)	0.057(6)	52

[a] Numbers in parentheses indicate standard error of the last significant digits. Amax values are determined at 388 nm.

RESULTS AND DISCUSSION

2-Ethylhexanoic acid is the most highly produced commercial aliphatic carboxylic acid (*3*). The ubiquitous use of this compound has led to extensive research into its toxicity. The purpose of this study was to examine the ability of cytochrome P450cam to produce 2-ethylhexanoic acid from 2-ethylhexanol. We were interested not only in its regioselective catalysis but also its inherent stereoselectivity, as each enantiomer shows different biological effects. The production of 2-ethylhexanoic acid is believed to involve two distinct oxidation reactions, as shown in Figure 3. Oxidation at the number one carbon position yields 2-ethyl-1,1-hexanediol as the intermediate compound leading to 2-ethylhexanoic acid production.

Substrate binding is an essential step in cytochrome P450 catalysis, displacing water as a sixth ligand and causing the iron to shift from a low to a high spin state. This shift in potential of the enzyme poises it for reduction, producing a marked spectroscopic change (*19*). These changes were measured for the natural substrate camphor and for (*R*)- and (*S*)-2-ethylhexanol and 2-ethylhexanoic acid. The results are shown in Table 1. The P450cam displays 2-fold higher affinity for (*R*)-2-ethylhexanol over the (*S*)- enantiomer as evidence by the spectral binding constant values (K_S). Also, the (*S*)- enantiomer converts a significantly higher percentage of the enzyme to the high spin state than the (*R*)-enantiomer under saturating conditions. Neither enantiomer converts 100% of the enzyme to high spin (*20*).

Steady-state initial velocity experiments were conducted on camphor, (*R*)-, and (*S*)-2-ethylhexanol. The results are listed in Table 2. While the K_m for (*S*)-2-ethylhexanol was found to be similar to that of (*R*)-2-ethylhexanol, the V_{max} was 3.5 times lower, corresponding to a 3-fold lower *V*/*K*. The differences in *V*/*K* imply a significant degree of specificity for (*R*)-2-ethylhexanoic acid production. Finally, 2-ethylhexanoic acid is produced at about 2% the rate of camphor. Studies with other aliphatic foreign substrates indicate similar efficiencies (*21*).

Table 2: Initial Velocity Experiments for 2-Ethylhexanoic Acid Production by Cytochrome P450cam

substrate	K_M (μM)	V_{MAX}[a]	V/K[b]
camphor	1.6(1)[c]	71(4)	44(3)
(R)-2-ethylhexanol	86(7)	1.3(1)	0.015(2)
(S)-2-ethylhexanol	68(1)	0.4(5)	0.0054(6)

[a] nmol/min/nmol. [b] μM/min. [c] Numbers in parentheses indicate standard error of the last significant digits.

The enantioselective properties of P450cam in single substrate experiments translate to racemic studies as well. Enantiomeric excess (EE) assays indicating a 2-fold higher (*R*)-2-ethylhexanoic acid production, (50% enantiomeric excess) are in agreement with the 3-fold higher *V*/*K* values relative to the (*S*)-enantiomer (Table 2).

To determine the regioselectivity of P450cam with 2-ethylhexanol, enzyme incubations were carried out at saturating conditions and examined for all possible metabolites. The results are listed in Table 3. As reported in the literature, P450cam produces solely (*R*)-5-exohydroxycamphor from (*R*)-camphor (*22*). Unlike camphor, four products were detected in both (*R*)- and (*S*)-2-ethylhexanol incubations with P450cam. Totaling all of the metabolites detected shows that (*S*)-2-ethylhexanol is turned over 1.4 times faster than the (*R*)-enantiomer. The enantiomers show differing amounts of product, with (*R*)-2-ethylhexanoic acid comprising 50% of product from the *R*-enantiomer and only 13% with the *S*-enantiomer. Interestingly, the 2-ethyl-1,2-hexanediol ratios differ in equal but opposite amounts. While the 1,4- and 1,5-diol formation occurs at more similar rates for both enantiomers. The presence of four products indicates that both enantiomers of 2-ethylhexanol have a degree of mobility in the active site, even though regio- and stereoselective catalysis is shown. The percent of 2-ethylhexanoic acid produced is not the final measure of efficiency for P450 mediated reactions, as water and hydrogen peroxide can also be produced (Figure 1.). High levels of these alternate products can decrease the efficiency of P450 as a biocatalyst. To examine these side reactions, hydrogen peroxide and water production were measured.

NADH consumption and coupling of wild-type P450cam for camphor and (*R*)- and (*S*)-2-ethylhexanol oxidations were measured. NADH serves as the initial electron donor in the reducing chain that provides the electrons for the catalytic cycle (*23*) (see Figure 1). Electrons are donated to P450cam in two steps to reduce molecular oxygen to an iron-peroxy intermediate. At this stage, hydrogen peroxide may be released from the enzyme. If hydrogen peroxide is not formed, molecular oxygen is cleaved to form one molecule of water and a reactive iron−oxygen complex. At this point the iron−oxygen complex can oxidize the substrate or be reduced by another two more electrons to form water (*24*). A number of possibilities exist that can account for poor turnover: (i) the substrate may bind in a nonproductive orientation. This will almost always result in increased water formation and NADH usage. (ii) The substrate may not bind strongly to the enzyme, slowing the overall catalytic cycle. (iii) The substrate may bind in an orientation that enhances hydrogen peroxide release, shunting the reducing equivalent away from product formation. The results of the stoichiometric studies are given in Table 4. Camphor turnover occurs with a high degree of coupling (92%), with the ratios of oxygen to NADH consumption near unity, agreeing with published values (*25*). Virtually no water formation is seen and the remaining reducing equivalents produce hydrogen peroxide.

The stoichiometry of 2-ethylhexanol catalysis differs dramatically. First, NADH consumption occurs at about 25% of the rate of camphor turnover, indicating poor binding of substrate and slow electron transfer. Furthermore, 2-ethylhexanol turnover only accounts for 5% of NADH consumption. The excess NADH consumption results in higher water and hydrogen peroxide formation rates as compared to camphor. Thus, it appears that the difference in turnover rates of camphor versus 2-ethylhexanol is due to two factors: slower NADH consumption and more peroxide and water formation. The ratio of NADH to oxygen for (*S*)-2-ethylhexanol is higher than for (*R*)-2-ethylhexanol. This indicates that more water is produced by the (*S*)-enantiomer. In contrast, the NADH consumption rates, substrate oxidation, and hydrogen peroxide formation are similar for the two enantiomers.

To elucidate structural factors that may cause this favorable production of (*R*)-2-ethylhexanoic acid, crystallographic studies were performed. P450cam crystals with (*R*)- and (*S*)-2-ethylhexanol were first attempted. However, the low

Table 3: Regioselectivity Data for Cytochrome P450cam Oxidation of 2-Ethylhexanol

	products				
	rates of products formation[a]				
substrate	2-ethylhexanoic acid	2-ethyl-1,2-hexane diol	2-ethyl-1,3-hexane diol	2-ethyl-1,4-hexane diol	total
(*R*)-2-ethylhexanol	1.30(2)[b]	0.33(3)	0.74(6)	0.21(5)	2.6(2)
(*S*)-2-ethylhexanol	0.47(1)	1.9(2)	1.0(1)	0.30(2)	3.6(2)

[a] nmol/min/nmol. [b] Numbers in parentheses indicate standard error of the last significant digits.

Table 4: Stoichiometric Rate Data for Cytochrome P450cam[a]

	substrates		products						
	NADH	O_2	ROH[b]	H_2O_2	H_2O	$NADH/O_2$	ROH/NADH	H_2O_2/NADH	H_2O/NADH
camphor	334(1)	316(12)	308(5)	28(6)	O(4)	1.06	0.92	0.08	0.00
(*R*)-2-ethylhexanol	86(2)	82(8)	3.5(3)	55(5)	15(3)	1.05	0.05	0.64	0.30
(*S*)-2-ethylhexanol	95(1)	57(8)	3.9(3)	53(7)	19(4)	1.67	0.05	0.56	0.42

[a] All rates are in nmol/min/nmol. [b] ROH describes the rate of total hydroxulated product, with 2-ethylhexanoic acid accounting for 2 NADH equiv.

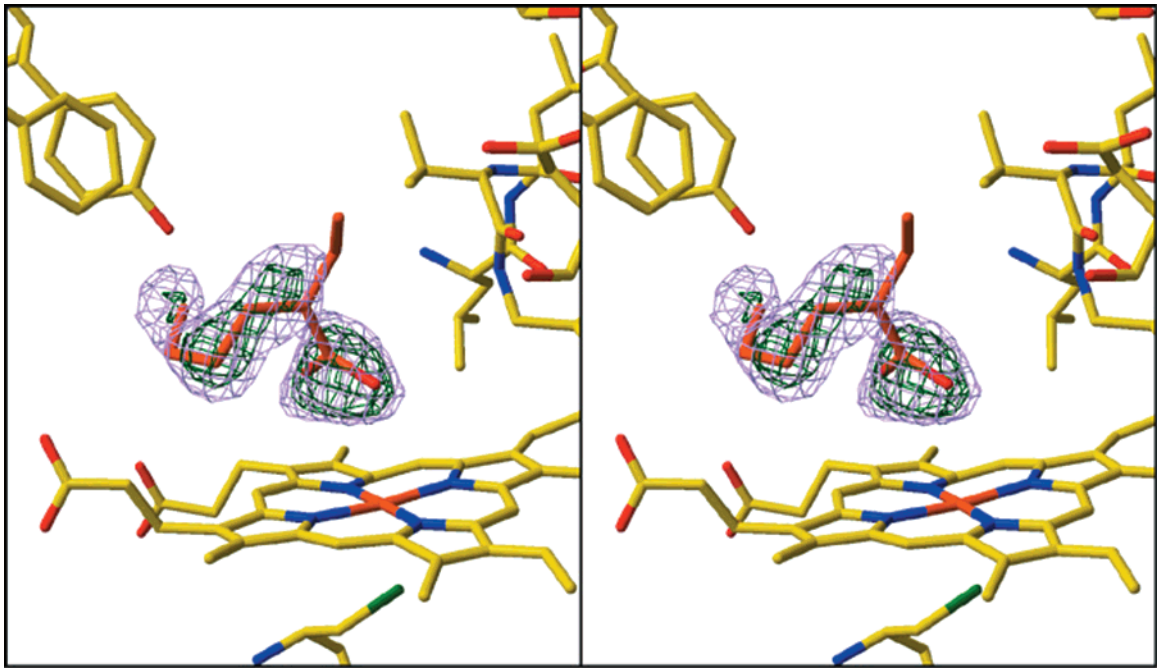

FIGURE 4: $2F_O-F_C$ omit maps of wild-type P450cam with either (*R*)-2-ethylhexanoic acid. Both images are at 2σ resolution.

solubility of these substrates made cocrystallization impossible. The sodium salts of 2-ethylhexanoic acid are much more soluble and were used instead. The statistics of refinement and data collection are given in supplemental information. A SA Omit map of (*R*)-2-ethylhexanoic acid in the active site is shown in Figure 4. Appearing directly above the heme is the density corresponding to (*R*)-2-ethylhexanoic acid, with what appears to be the carboxylate group closest to the iron atom. Moving toward the rear of the image appears to be the aliphatic chain of the substrate, coming in close contact with Y96 and F87. On the basis of the best fit model the ethyl side chain of the substrate seems to be pointing up and away from the heme, closely interacting with L244. Finally, the density does not perfectly fit the substrate. This is likely to be a results of the multiple binding orientations required for the multiple products reported in Table 3. For (*S*)-2-ethylhexanoic acid there is no uniform density in the active site or close to the heme, which could indicate a high degree of disorder or that in fact no ligand is bound (data not shown). Such a hypothesis would lead to the idea that (*R*)-2-ethylhexanol would be productively poised for oxidation while the (*S*)- enantiomer would have no definite position, leading either to a wide variety of metabolites or complete lack of turnover. The results of these studies are consistent with the more favorable positioning of the (*R*)-enantiomer versus the (*S*)-enantiomer which may contribute to the stereoselective differences seen above.

While much information can be attained from crystallographic studies, short-lived intermediates in a reaction, such as the transition state of hydrogen atom abstraction, are difficult or impossible to measure. Therefore, we performed ab initio quantum mechanical calculations to elucidate the structure and energetics of the transition state in P450-catalyzed reactions. Because the heme-oxy species is too large to include in these calculations, we replaced it with the methoxy radical, which has been shown to behave similarly (*26*). Hydrogen atom abstraction transition states were determined on three unique carbons of 2-ethylhexanol. The transition states and their corresponding activation energies are listed in Figure 5. Transition states were optimized for three sites of hydrogen atom abstraction: the primary carbon with the alcohol group, the primary carbon on the opposite end of the chain, and the tertiary carbon with the single hydrogen. Since these calculations are done in an achiral environment the results are not enantioselective. Abstraction from the hydroxylated carbon gives the lowest activation barrier, indicating that the 2-ethylhexane-1,1-diol should be the most favorable product, followed by the 1,2-diol. Abstraction from the opposite end of the substrate leading to the primary radical, i.e., the #6 methyl carbon, gave the highest energy barrier. These quantum mechanical calculations indicate that, based upon electronic factors alone, 2-ethylhexanoic acid should be the primary product of 2-ethylhexanol catalysis by cytochrome P450cam followed by 1,2-diol formation. The fact that we see different product distributions for (*R*)- and (*S*)-2-ethylhexanol as shown in Table 3 indicates some role of the protein in determining the regioselectivity of reaction. Thus, it appears that 2-ethylhexanol catalysis is governed by both structural and electronic factors.

To further elucidate the structural features that effect catalysis, we have combined molecular dynamic simulations whose structural information was obtained from crystallographic data with the ab initio quantum mechanical transition state reported above. Depicted in Figure 6 is each transition state leading to 2-ethyl-1,1-diol production. While both transition states share similar positioning of the main chain and ethyl group, the difference between the (*S*)- and the (*R*)-enantiomer causes a shift of the hydroxyl group of the (*R*)-enantiomer toward the hydroxyl groups of tyrosine 96 and threonine 101 by 0.7 and 0.9 Å, respectively. These electrostatic interactions could help to hold the (*R*)-enantiomer in a favorable position for oxidation to the acid. In contrast, the (*S*)-enanatiomer has the alcohol oxygen pointing toward T252 (see Figure 6), an important residue in the proton shuttle that produces and stabilizes the oxygen

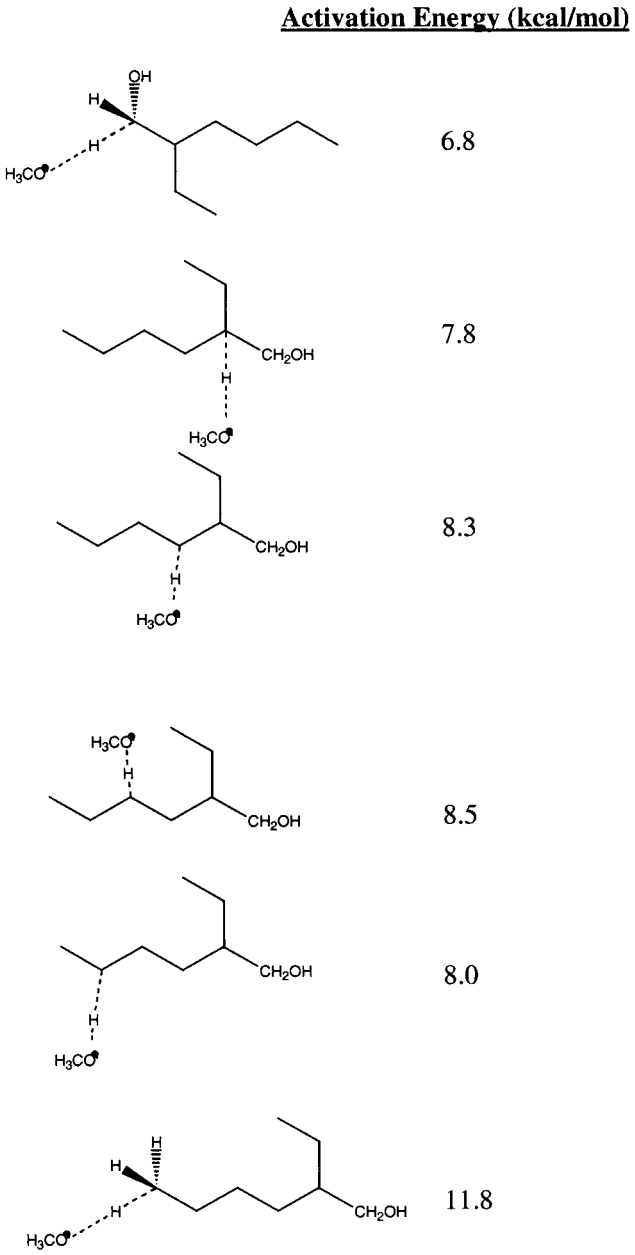

FIGURE 5: Ab initio transition state calculations and corresponding activation energies.

intermediates. The results summarized in Table 4 imply two possible substrate conformations for each enantiomer: one where the number 1 carbon is poised over the heme and the other with the opposite end of the aliphatic chain is near the iron-oxo species. Oxidation at the number 1 or 2 carbon results in either 2-ethylhexanoic acid or 2-ethyl-1,2-hexanediol. Hydroxylation at the opposite end yields 2-ethyl-1,3-hexanediol, 2-ethyl-1,4-hexanediol, 2-ethyl-1,5-hexanediol, or 2-ethyl-1,6-hexanediol. Formation of 2-ethyl-1,2-hexanediol could result from hydrogen bond formation between tyrosine 96 and the alcohol oxygen of 2-ethylhexanol. Removing this hydrogen bond donor could eliminate this byproduct, increasing the percent of 2-ethylhexanoic acid produced. Wong and co-workers have shown this to be true for alkane hydroxylation (*21*). Finally, T185 and V396 interact with the ethyl group during catalysis, and altering these groups by mutagenesis might alter the regio- and stereoselectivity of the enzyme. One final possibility is that

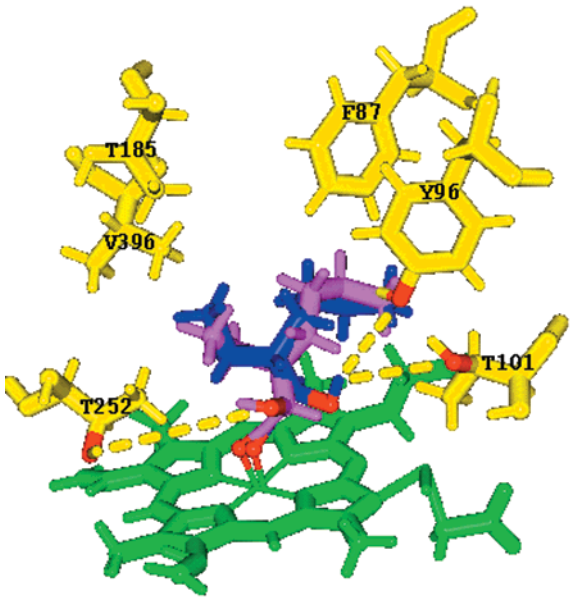

FIGURE 6: (*S*)-2-Ethylhexanol (in magenta) and (*R*)-2-ethylhexanol (in blue) transition states from molecular dynamics studies. Potentially important oxygen atoms are shown in red, significant active site amino acid residues in yellow, and heme in green. Possible hydrogen bond interactions are shown as dotted lines.

T252 could be mutated and the hydroxyl group of the substrate used to guide proton transfer in a similar fashion as substrate for P450eryF (REF).

This mutagenesis approach could of course be applied to other residues as well. Increasing side chain volume has a second benefit of decreasing active site volume, which should place the substrate in closer contact with the heme, resulting in increased substrate oxidation and decreased hydrogen peroxide and water formation. Sligar has achieved this with ethylbenzene oxidation (*27*). Thus, the data provided in this paper can serve as a template for improving 2-ethylhexanoic acid production.

SUPPORTING INFORMATION AVAILABLE

Data collection information and refinement statistics for 2-EHXA-P450cam complexes. This material is available free of charge via the Internet at http://pubs.acs.org.

REFERENCES

1. Testa, B. (1995) in *Biochemistry of Redox Reactions* (Testa, B., Ed.) pp 70−121, Academic Press, New York.
2. Mueller, E. J., Loida, P. J., and Sligar, S. G. (1995) in *Cytochrome P450: Structure, Mechanism, and Biochemistry* (Montellano, P. R. O. d., Ed.) pp 83−124, Plenum Press, New York.
3. Riemenschneider, W. (1986) *Ullmann's Encyclopedia of Industrial Chemistry A5*, 235−248.
4. Kluwe, W. M. (1982) *Env. Health Perspect. 45*, 1.
5. Jaeger, R. J., and Rubin, R. J. (1972) *New Eng. J. Med. 287*, 1114−1118.
6. Albro, P. W., Corbett, J. T., Schroeder, J. L., Jordan, S., and Matthews, H. B. (1982) *Env. Health Perspect. 45*, 19−25.
7. Sundberg, C., Wachtmeister, C., Lundgren, B., and DePierre, J. W. (1994) *Chirality 6*, 17−24.
8. Collins, M. D., Scott, W. J., Miller, S. J., Evans, D. A., and Nau, H. (1992) *Toxicol. Appl. Pharm. 112*, 257−265.
9. Macherey, A. C., Gregoire, S., Tainturier, G., and Lhuguenot, J. C. (1992) *Chirality 4*, 478−483.
10. Shimoji, M., Yin, H., Higgins, L., and Jones, J. P. (1998) *Biochemistry 37*, 8848−52.

11. Gunsalus, I. C., and Wagner, G. C. (1978) *Methods Enzymol. 52*, 166−188.
12. Otwinowski, Z., and Minor, W. (1997) *Methods Enzymol. 276*, 307−326.
13. Schlichting, I., Berendzen, J., Chu, K., Stock, A. M., Maves, S. A., Benson, D. E., Sweet, R. M., Ringe, D., Petsko, G. A., and Sligar, S. G. (2000) *Science 287*, 1622.
14. Pannu, N. S., and Read, R. J. (1996) *Acta Crystallogr. A52*, 659−668.
15. Brunger, A. T., Adams, P. D., Clore, G. M., DeLano, W. L., Gros, P., Grosse-Kunstleve, R. W., Jiang, J.-S., Kuszewski, J., Nilges, M., Pannu, N. S., Read, R. J., Rice, L. M., Simonsen, T., and Warren, G. L. (1998) *Acta Crystallogr. D54*, 905−921.
16. Frisch, M. J. e. a. (1995) Gaussian, Inc., Pittsburgh, PA.
17. Bayly, C. I., Cieplak, P., Cornell, W. D., and Kollman, P. A. (1993) *J. Phys. Chem. 97*, 10269−10280.
18. Jones, J. P., and Korzekwa, K. R. (1996) *Methods Enzymol. 272*, 326−35.
19. Sligar, S. G. a. G., and I. C. (1976) *Proc. Natl. Acad. Sci. U.S.A. 73*, 1078−1082.
20. Yu, C., Gunsalus, I. C., Katagiri, M., Suhara, K., and Takemori, S. (1974) *J. Biol. Chem. 249*, 94−101.
21. Stevenson, J., Westlake, A. C. G., Whittock, C, and Wong, L. (1996) *J. Am. Chem. Soc. 118*, 12846−12847.
22. Cushman, D. W., Tsai, R. L., and Gunsalus, I. C. (1967) *Biochem. Biophys. Res. Commun. 26*, 577.
23. Gunsalus, I. C., Pederson, T. C., and Sligar, S. G. (1975) *Annu. Rev. Biochem. 44*, 377.
24. Loida, P. J., and Sligar, S. G. (1993) *Biochemistry 32*, 11530−11538.
25. Atkins, W. M., and Sligar, S. G. (1987) *J. Am. Chem. Soc. 109*, 3754−3760.
26. Manchester, J. I., Dinnocenzo, J. P., Higgins, L. A., and Jones, J. P. (1997) *J. Am. Chem. Soc. 119*, 5069−5070.
27. Loida, P. J., and Sligar, S. G. (1993) *Protein Eng. 2*, 207−212.

BI010063+